



# Engineering of a Substrate Affinity Reduced S-Adenosyl-methionine Synthetase as a Novel Biosensor for Growth-Coupling Selection of L-Methionine Overproducers

Jianfeng Huang<sup>1,2</sup> · Jinhui Liu<sup>1,3</sup> · Huaming Dong<sup>1,4</sup> · Jingjing Shi<sup>1,2</sup> · Xiaoyan You<sup>1,3</sup> · Yanfei Zhang<sup>1,2</sup> 

Accepted: 9 December 2023 / Published online: 27 December 2023

© The Author(s), under exclusive licence to Springer Science+Business Media, LLC, part of Springer Nature 2023

## Abstract

Biosensors are powerful tools for monitoring specific metabolites or controlling metabolic flux towards the products in a single cell, which play important roles in microbial cell factory construction. Despite their potential role in metabolic flux monitoring, the development of biosensors for small molecules is still limited. Reported biosensors often exhibit bottlenecks of poor specificity and a narrow dynamic range. Moreover, fine-tuning the substrate binding affinity of a crucial enzyme can decrease its catalytic activity, which ultimately results in the repression of the corresponding essential metabolite biosynthesis and impairs cell growth. However, increasing intracellular substrate concentration can elevate the availability of the essential metabolite and may lead to restore cellular growth. Herein, a new strategy was proposed for constructing whole-cell biosensors based on enzyme encoded by essential gene that offer inherent specificity and universality. Specifically, S-adenosyl-methionine synthetase (MetK) in *E. coli* was chosen as the crucial enzyme, and a series of MetK variants were identified that were sensitive to L-methionine concentration. This occurrence enabled the engineered cell to sense L-methionine and exhibit L-methionine dose-dependent cell growth. To improve the biosensor's dynamic range, an S-adenosyl-methionine catabolic enzyme was overexpressed to reduce the intracellular availability of S-adenosyl-methionine. The resulting whole-cell biosensor effectively coupled the intracellular concentration of L-methionine with growth and was successfully applied to select strains with enhanced L-methionine biosynthesis from random mutagenesis libraries. Overall, our study presents a universal strategy for designing and constructing growth-coupled biosensors based on crucial enzyme, which can be applied to select strains overproducing high value-added metabolites in cellular metabolism.

**Keywords** Whole-cell biosensor · Crucial enzyme · L-Methionine · S-Adenosyl-methionine synthetase · Growth-coupled selection

---

Jianfeng Huang and Jinhui Liu contributed equally to this work.

---

Extended author information available on the last page of the article

## Introduction

Expanding industrialization brings about various global issues such as the depletion of fossil resources, climate change, and environment pollution. Biomanufacturing, which involves the production of chemicals from renewable resources, has emerged as a promising alternative that is considered more effective, environmentally friendly, and sustainable [1–3]. The core of biomanufacturing is the construction of high-performance microbial cell factories, which can be manipulated by rewiring the cellular metabolism in chassis cell based on synthetic and systems biology methodology to improve the titer, yield, and productivity [4]. However, due to the complexity of cellular metabolism, our understanding toward the potential impacts of unintuitive factors on the metabolic flux towards the target chemicals is still limited. Thus, the rational design of microbial cell factories for the production of high-value chemicals is still a time-consuming and labor-intensive process by using conventional metabolic engineering strategies [1, 5]. Genetically encoded biosensors are powerful tools that can help to overcome the aforementioned limitations by monitoring the intracellular contents of metabolites and transmitting them into detectable signals such as fluorescence, antibiotic resistance, and growth phenotype [6–12]. Despite their usefulness, biosensors for valuable chemicals, including natural intermediates in the metabolic network, are still limited [10]. Therefore, it is crucial to develop biosensors that can facilitate effectively high-throughput screening/selection of valuable chemical overproducers with superior performance from libraries containing large number of mutants.

Crucial enzymes involved in the biosynthesis of vital metabolites exist widely in the complex biological system [13]. Some of the intermediates in the biosynthetic pathways of essential metabolites are also considered high-value chemicals, such as those found in amino acids, vitamins, and shikimic pathways [14, 15]. Studies have reported that the active pocket of crucial enzyme can be fine-tuned through rational design to disrupt the interactions between intermediates and active residues, without impacting cofactor binding [16, 17]. The intracellular availability of the target intermediate was then positively related to cell growth [18, 19]. Therefore, modifying crucial enzymes as biosensors to monitor the target chemical with cell growth as a readout could be a promising approach for selecting overproducing strains of valuable chemicals. Compared to conventional biosensors based on transcription factors, DNA/RNA aptamers or allosterically regulated proteins [6–12], the crucial enzyme-based biosensor is a novel type of biosensor with inherent specificity suitable for detecting metabolic intermediates that were previously untraceable.

Methionine is a sulfur-containing amino acid that is essential and widely utilized in the pharmaceutical and animal feed industries, with an annual demand over a million tons, while historically methionine was mainly produced by chemical synthesis using toxic raw materials such as methanethiol, hydrocyanic acid, and acraldehyde. Despite the recent advancement of a fermentation-enzymatic process for L-methionine production [20, 21], producing methionine entirely from clean and sustainable sources remains a significant challenge. This is due to the complexity of L-methionine biosynthesis and multi-layer regulation, which makes it difficult to optimize the metabolic flux towards L-methionine by using traditional metabolic engineering strategies [20]. The construction of a high-performing L-methionine producing strain also requires the manipulation of dozens of genes, which further complicate the process [20, 22, 23]. To overcome this obstacle, several biosensors have been developed to aid in the screening and isolation of L-methionine overproducers from microbial mutation libraries [24]. A biosensor was constructed using a transcriptional regulator Lrp and a regulated fluorescent gene to detect and quantify the

intracellular contents of L-methionine and branched-chain amino acids in *Corynebacterium glutamicum*. However, Lrp has poor specificity [25], which is a common issue with transcription factor-based biosensors, as it increases the risk of false positive and limits its further application. A nanosensor was developed using methionine binding protein (MetN) from *E. coli* to specifically sense the L-methionine and output a fluorescence resonance energy transfer (FRET) signal with a calculated affinity ( $K_d$ ) reaching up to 203  $\mu\text{M}$  [26]. However, the FRET-based biosensor has a weak signal intensity and requires a highly sensitive equipment for the signal detection, limiting its wide application. Although biosensors based on the aminoacyl-tRNA synthetase [17] and rare codon-rich selection marker [27] have been reported, their applications are restricted to the selection of amino acid overproducers, excluding L-methionine. Hence, it is crucial to propose a new strategy for designing biosensors that can facilitate the development of L-methionine overproducing strains.

The primary aim of this study is to propose a newly universal strategy for designing and constructing whole-cell biosensors capable of detecting small molecules, such as L-methionine, that lack natural transcription factors and riboswitches. The biosensor is designed by using an affinity reduced crucial enzyme that couples the production of target small molecule with the growth of the cell. Using *E. coli* S-adenosyl-methionine synthetase (MetK) as an example, a genomic *metK* deleted *E. coli* was constructed, as well as a process for biosensor assessment was established. On this basis, a set of affinity reduced MetK-based whole-cell biosensors that exhibit the inherent specificity and universality, with cell growth serving as the readout, were constructed and tested. In addition, a strategy for extending the dynamic range of the biosensors was proposed and demonstrated. Furthermore, the preferred biosensor was successfully applied to identify mutants with increased L-methionine-producing capacity from the random mutagenesis library. Our findings offer a promising approach for developing crucial enzyme-based whole-cell biosensors for valuable chemicals in the cellular metabolism, which could accelerate the development of cell factories.

## Material and Methods

### Enzymes and Chemicals

The Phusion High-Fidelity DNA polymerase and the CloneExpress® II One Step Cloning Kit were purchased from Vazyme (Nanjing, China). The E.Z.N.A.® Plasmid DNA Mini Kit I and the E.Z.N.A.® Gel Extraction Kit were purchased from Omega (Georgia, USA). AxyPrep PCR purification Kit was purchased from Axygen (California, USA). Oligonucleotides were synthesized by Tsingke (Beijing, China). L-Methionine and other amino acids were purchased from Sigma (Missouri, USA). Antibiotics were purchased from Sangon Biotech (Shanghai, China). Other chemicals of higher analytical grade are not specified in this study.

### Media and Culture Condition

The cultivation medium LB (Lysogeny Broth) was composed of 10 g/L tryptone, 5 g/L yeast extract, and 10 g/L NaCl. The LB agar plates were prepared by adding 2% agar powder to liquid LB medium. The M9 minimal salt medium (containing 0.24 g/L  $\text{MgSO}_4$ , 11.1 mg/L  $\text{CaCl}_2$ , 6.8 g/L  $\text{Na}_2\text{HPO}_4$ , 3.0 g/L  $\text{KH}_2\text{PO}_4$ , 0.5 g/L NaCl, and 1.0 g/L  $\text{NH}_4\text{Cl}$ ) supplemented with 20 g/L glucose (termed as M9 medium) was used for growth test of

mutant strains. The fermentation medium SC-M9 contains additional 20 g/L glucose, 2 g/L  $\text{Na}_2\text{S}_2\text{O}_3$ , 10 g/L  $\text{CaCO}_3$ , 61 mL/L amino acid mixture, 0.1 g/L Vb1, and 2 mg/L Vb12 in the M9 salty solution. Each amino acid derived from the amino acid mixture containing Thr, Ser, Gly, Pro, Ala, Arg, Cys, Val, Ile, His, Gln, Asn, Leu, Glu, and Trp in SC-M9 was achieved to a final concentration of 0.1 g/L. Antibiotics were used according to the resistance of strain at the following concentrations: kanamycin (Kan) 50 mg/L, spectinomycin (SD) 50 mg/L, chloramphenicol (Cm) 34 mg/L, and streptomycin (Sm) 50 mg/L. Specifically, the chloramphenicol (Cm) was dissolved in ethanol. For conventional strain culture, cells were cultivated at 37 or 30 °C in tube and/or flasks shaking at 220 rpm. For growth test, cells were cultivated at 37 °C in 50-mL tube containing 10 mL test medium shaking at 220 rpm, or in 24-well plates with each well containing 1 mL test medium shaking at 800 rpm in MicroScreen HT (Tianjin, China).

## Plasmid Construction

Plasmids and primers used are listed in Table S1 and Table S2, respectively. The plasmid construction scheme was exhibited in Figure S1. Molecular cloning and plasmid construction were performed within *E. coli* DH5 $\alpha$ . *E. coli* MG1655 derivatives were used for biosensor characterization and L-methionine overproducer screening. Plasmid pTarget-donor-*metK*\* was constructed to knockout the essential gene *metK* from the *E. coli* MG1655 genome. Primer pair pT-*metK*-F/pT-*metK*-R was used to amplify the pTargetF backbone to mutant N<sub>20</sub> sequence for the construction of the basic plasmid pT-N<sub>20metK</sub>. The pT-N<sub>20metK</sub> backbone was amplified with primers pT-donor-F/pT-donor-R. The 500 bp upstream and the 500 bp downstream of *metK* were amplified from *E. coli* MG1655 genomic DNA with primers *metK*-LA-F/*metK*-LA-R and *metK*-RA-F/*metK*-RA-R. These three PCR fragments were ligated to generate plasmid pT-donor. Since *metK* is an essential gene and cannot be directly deleted from the *E. coli* MG1655 genome, the *metK* gene with the RBS sequence (5'-AAGGAGATATAC-3') was cloned into the plasmid pT-donor to construct the plasmid pTarget-donor-*metK*. At the same time, the PAM (protospacer adjacent motif, 5'-CCT-3') of *metK* was mutated to 5'-TCT-3' to prevent the cleavage of *metK* on the pTarget-donor-*metK*\* by Cas9. For pTarget-donor-*metK*\* construction, pT-donor backbone and *metK* fragment with RBS and PAMless mutation were amplified by primer pair PND-*metK*\*-F/PND-*metK*\*-R and RBS-*metK*\*-F/RBS-*metK*\*-R, respectively. And then, the two PCR fragments were ligated to generate plasmid pTarget-donor-*metK*\*.

A complementary plasmid pC-*metK*\* was constructed to maintain the cell growth of the genomic *metK* deleted strain after the curing of the CRISPR-Cas9 plasmids. The backbone and *metK* cassette were amplified by using primer pair MP6-F/MP6-R and *metK*-F/*metK*-R from MP6 plasmid and *E. coli* MG1655 genome, respectively, and then, two fragments were ligated to generate basic plasmid pC-*metK*. Then, the same mutation on selected PAM site of *metK* as pTarget-donor-*metK*\* was introduced using primers *metK*\*-F/*metK*\*-R to obtain plasmid pC-*metK*\*. In order to improve the replacement efficiency, the FIp/FRT site-specific recombination system was introduced on the basis of plasmid incompatibility. The backbone of the plasmid and *metK*\* cassette with an FRT site was amplified with primers ORI-F/ORI-R and MetK-F/MetK-R from plasmid pC-*metK*\*, respectively, and the Kan resistance fragment with an FRT site was obtained with primers Kan-F/Kan-R by using pET28a(+) as template. The three fragments were ligated to generate the rescue plasmid pC-FRT-*metK*\*.

For the construction of growth-coupled biosensor capable of responding to L-methionine, the plasmid backbone and wild-type *metK* cassette were amplified using primers CDFD-F/CDFD-R and CmetK-F/CmetK-R from plasmid MP6 [28] and *E. coli* MG1655 genome, respectively. And then, the two fragments were ligated to generate plasmid pHL1. The pHL1 backbone was amplified using primer pair CDFD1-F/CDFD1-R, and Flp fragment was amplified with primers FLP-F/FLP-R from pCP20 [29]. Two fragments were ligated to generate basic biosensor plasmid pHL4. For E55, Q98, D238, and K269 that interact with L-methionine were mutated through site saturation mutagenesis by using primers E55X-F/R, Q98X-F/R, D238X-F/R, and K269X-F/R (X refers to the other 19 amino acids, Table S1) and using plasmid pHL4 as a template. Eventually, a biosensor library containing 217 mutants carrying single or combinational mutations was obtained. For overexpression of S-adenosyl-homocysteine nucleosidase encoded by *mtnN* involved in S-adenosyl-L-methionine catabolism, the backbone and *mtnN* fragment were amplified with primers tNC-F/tNC-R and *mtnN*-F/*mtnN*-R from pHL4 and *E. coli* MG1655 genomic DNA. Two fragments were ligated by using One Step Cloning Kit to generate plasmid pHL7.

## Genetic Modification of the Host

All the strains used in this study are listed in Table S3. The *metK* was deleted from *E. coli* MG1655 genome to test the growth-coupling effects of the designed biosensors. In order to knockout *metK*, pCas and pTarget-donor-*metK*\* were transformed into *E. coli* MG1655 by electroporation according to the previous report [30]. Subsequently, *metK* knockout strains were screened in plates containing Kan and SD. The complementary plasmid pC-FRT-*metK*\* was transformed into the *metK* knockout strain to form a three-plasmid system to maintain the cell survival after the pT-donor-*metK*\* was eliminated. Next, the pCas and pTarget-donor-*metK*\* were eliminated orderly. Finally, the strain *E. coli* MG1655  $\Delta metK/pC-FRT-metK^*$  named HL<sub>b</sub>2 was obtained. To construct the starting strain for random genomic mutagenesis, the L-methionine transporter encoding gene *metD* was deleted from *E. coli* MG1655 genome to obtain *E. coli* MG1655  $\Delta metK \Delta metD/pC-FRT-metK^*$  named HL<sub>b</sub>3 for further study.

## Plasmid Replacement

In order to replace the rescue plasmid, the biosensor plasmid was transformed into HL<sub>b</sub>2 competent cells. After incubation for 2 h, the cells were collected by centrifugation at 5000 rpm for 5 min. The cells were resuspended and inoculated into M9 medium containing 0.8 g/L L-methionine, cultured at 37 °C, 220 rpm. The grown cells were diluted  $10^{-3} \sim 10^{-6}$  and spread onto LB plates containing 50 mg/L Sm, and cultured at 37 °C overnight. Ten to twenty single clones were randomly picked from the Sm plate and streaked on the Kan plate to verify whether the rescue plasmid had been replaced. Subsequently, two single clones without Kan resistance were randomly selected and inoculated into 10 mL LB medium, and the plasmids were extracted and sequenced to verify whether *metK* had a reverse mutation (Table S4-7).

## Growth Assay

Cells were cultured to stationary phase in LB medium. The cells were resuspended by using M9 medium after centrifugation, and then inoculated into M9 medium with an initial OD<sub>600</sub> of 0.02. Cells were inoculated into 10 mL M9 medium with or without 0.8 g/L L-methionine, respectively, and cultivated at 37 °C, 220 rpm for 12 h to test growth-coupling effect of cell harboring biosensor plasmid. Different final concentrations of L-methionine (0, 0.008, 0.08, 0.8 g/L) were added to M9 medium to test the response of cell growth to L-methionine supplementation. To monitor the cell growth, 50 μL of the culture was taken at a period of time and diluted to 200 μL with ddH<sub>2</sub>O in a 96-well microplate. OD<sub>600</sub> was measured using a microplate reader (TEKAN, Switzerland). The specific growth rate,  $\mu$ , at the different times of sampling was estimated from the OD<sub>600</sub> growth curve using five consecutive OD<sub>600</sub> measurements according to the formula [31] below:

$$\mu = \frac{\Delta \ln OD_{600}}{\Delta t},$$

where  $t$  is time.

## Quantitative Real-Time PCR and Data-Independent Acquisition Mass Spectrometry

HL<sub>b</sub>4 and HL<sub>b</sub>32 were grown in 10 mL LB medium for 16 h at 37 °C (two biological replicates per strain). Then, strains were inoculated to an OD<sub>600</sub> of 0.02 in 10 mL M9 medium containing 1 g/L L-methionine and grown until an OD<sub>600</sub> of 0.6 was reached. One thousand cells/strain were harvested for RT-PCR using Single Cell Sequence Specific Amplification Kit purchased from Vazyme (Nanjing, China) according to the manufacturer's protocol. qPCR was performed using Roche LC96 (Roche) and ChamQ Universal SYBR qPCR Master Mix purchased from Vazyme (Nanjing, China) according to the manufacturer's protocol. Briefly, each reaction contained a final volume of 20 μL (10 μL 2×ChamQ Universal SYBR qPCR Master Mix), 0.4 μL of each primer (10 mM), 9.2 μL nuclease-free water, and 1 μL diluted cDNA as recommended by the protocol of Single Cell Sequence Specific Amplification Kit produced by Vazyme (Nanjing, China). Each sample was tested in triplicate using the recommended program in manufacturer's protocol. 16S rRNA was used as reference gene. CT values of 16S rRNA and *metK* were calculated by LightCycler® 96 SW 1.1 for further dCT, ddCT, and 2<sup>-ΔΔCT</sup> (fold change) calculation. For the data-independent acquisition mass spectrometry assay, HL<sub>b</sub>4 and HL<sub>b</sub>32 were inoculated to an OD<sub>600</sub> of 0.02 in 10 mL M9 medium containing 1 g/L L-methionine and grown until an OD<sub>600</sub> of 0.6 was reached. Ten OD<sub>600</sub> cells were harvested for further quantification using AB Sciex 5600 Triple TOF system (AB Sciex, USA) according to the previous report [32].

## Selection of L-Methionine Overproducers from ARTP Randomly Mutated Libraries

The strain HL<sub>b</sub>3 was employed for random mutagenesis using the ARTP (atmospheric and room-temperature plasma) [33] mutation system. One milliliter of the culture (OD<sub>600</sub> = 0.6–0.8) was centrifuged and resuspended with normal saline, and was separated to metal slide by taking 10 μL cells suspension. Next, the metal slide was exposed to helium flow for 0 s, 15 s, 30 s, 45 s, 90 s, and 120 s with fatality rate

of 0, 21.03, 56.60, 97.96, 99.99, and 99.99%, respectively. The treated mutants were washed with 1 mL of LB medium and transferred to a 1.5-mL sterile centrifuge tube for 2 h incubation. Then, 500  $\mu\text{L}$  of the culture was inoculated into 50 mL of LB until the  $\text{OD}_{600}$  reached 0.4–0.6. The competent cells were made and transformed with preferred biosensors by electroporation for further L-methionine overproducer selection. The transformants were incubated for 2 h and then transferred to M9 medium, allowing L-methionine overproducing strains to be selected and enriched by the optimal biosensors under conditions containing glucose as the sole carbon source. When the strain gained a specific fast growth, the culture was diluted properly and about 1000 cells (estimated by  $0.8 \times 10^8$  cells/ $\text{OD}_{600}/\text{mL}$ ) [34] were spread on SC-M9 plates containing 50 mg/L Sm. The L-methionine production capacities of the colonies with larger size were further tested by HPLC.

### L-Methionine Production Test and HPLC Analysis

To test the L-methionine productivity of the mutants, colonies were picked from the SC-M9 plate and inoculated into 10 mL LB medium. The overnight culture was inoculated into SC-M9 medium containing 10 g/L  $\text{CaCO}_3$  at 1% inoculum, and cultured at 37 °C. For flask fermentation, the overnight culture of single colony was inoculated into 500-mL shake flask containing 100 mL of SC-M9 medium and individually sterilized 10 g/L  $\text{CaCO}_3$ , and cultured for 48 h at 37 °C, 220 rpm. To evaluate the L-methionine production capacity of the mutants, the cultures were centrifuged at 12,000 rpm for 2 min. Subsequently, 100  $\mu\text{L}$  of the supernatant was mixed with 100  $\mu\text{L}$  of  $\text{NaHCO}_3$  and 100  $\mu\text{L}$  of 2,4-dinitrofluorobenzene (1:100 v/v in acetonitrile) and the reaction mixture was incubated for 1 h at 60 °C. Finally, 700  $\mu\text{L}$  of PBS was added to stop the reaction. The concentration of L-methionine in the supernatant was quantitatively analyzed by using HPLC equipped with a 2998 UV detector (Waters, USA) and a Waters X Bridge C18 column (5  $\mu\text{m}$ , 150  $\times$  4.6 nm) [22].

## Results

### Design Principle of Crucial Enzyme-Based Biosensors

Microorganisms require crucial enzymes for the biosynthesis of essential metabolites such as vitamins and amino acids, which are important for bacterial survival [35]. The affinity of crucial enzymes towards substrate can be reduced by engineering the substrate binding site of enzymes. Under appropriate culture condition, this modified crucial enzyme can produce the required metabolite efficiently, depending on the increased availability of the corresponding substrate (Fig. 1A (a–c)). This feature of the crucial enzyme variants can be leveraged to develop growth-coupled biosensors by selecting the overproducing strains of highly value chemicals (Fig. 1A (d)). To this end, the original genomic copy of an essential gene is disrupted and a complementary plasmid carrying the same essential gene is transformed to maintain the cell growth. This parental strain is used for the construction of the mutant library. Next, a plasmid containing essential gene variant is transformed to replace the complementary plasmid, and this occurrence enables the characterization of the crucial enzyme mutants and isolation of overproducing strains (Fig. 1B). Using this approach, the risk of reverse mutation of the mutant encoded by essential gene in the biosensor during

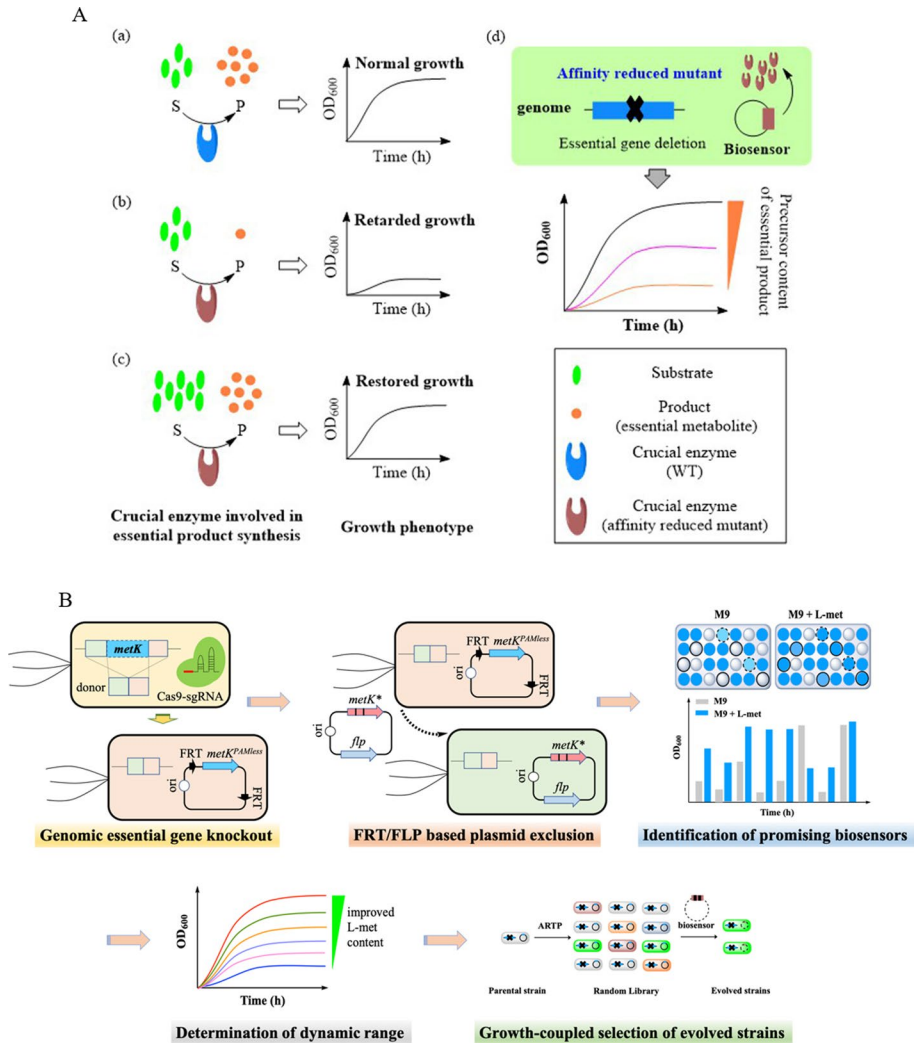


**Fig. 1** Schematic diagram of developing crucial enzyme-based biosensor and selection of overproducer from random library. **A** Synthesis of the essential metabolites in normal cells (a). The low affinity mutants of a crucial enzyme cannot produce enough corresponding essential metabolite which retards the cell growth (b). Increased intracellular availability of the cognate substrate restores synthesis of essential metabolite and cell growth (c). A sensor cell with genomic essential gene disrupted carrying a low affinity variant in complementary plasmid grows significantly faster in M9 medium supplemented with elevated concentration of substrate (d). **B** Schematic representation of the procedure for the screening, characterization of the crucial enzyme-based biosensor, and its application in L-methionine overproducer selection from random library prepared by ARTP (atmospheric and room-temperature plasma)

microbial mutant library preparation can be minimized. The identified crucial enzyme mutant with reduced affinity towards the cognate substrate can be further used for biosensor characterization and overproducer isolation.



## Construction of MetK-Based Biosensor for Proof of Principle

In *E. coli*, S-adenosyl-methionine (SAM) is produced exclusively by S-adenosyl-methionine synthetase, which is encoded by *metK*. SAM is the most widely used methyl donor in transmethylation, transsulfuration, and polyamine synthesis [36]. To develop a biosensor for L-methionine detection in *E. coli*, a variant of S-adenosyl-methionine synthetase with reduced substrate binding affinity was engineered as a proof of concept.

The primary challenge in constructing the MetK-based whole cell biosensor was to perform an in-frame knockout of the genomic copy of *metK*. A complementary plasmid carrying wild-type *metK* expression cassette was pre-transformed into *E. coli* MG1655 to maintain the normal growth when its genomic *metK* was disrupted. To prevent Cas9 from targeting to wild-type *metK* in the complementary plasmid and to obtain only the complementary plasmid (pTarget-donor-*metK*\*) for gene knock-out, a mutated version of the PAM recognition site was introduced into *metK*, named as *metK*\* (see the “Material and Methods” section). To prevent *metK*\* in pTarget-donor-*metK*\* plasmid from functioning as a patch with significantly higher efficiency than the designed donor DNA fragment during homology-directed repair, the spacer sequence (N<sub>20</sub>) was shifted to a restricted window. This shift of less than 30 bp from the end of the target fragment ensures the expected Red recombination by using the designed donor as the patch [37, 38] (Fig. S2A). Combining of these two strategies led to a significant improvement in the efficiency of gene deletion, which reached up to 100% (Fig. S2B). Finally, pC-*metK*\* was transformed to cure pCas and pTarget-donor-*metK*\* as previously described [30]. The resultant strain HL<sub>b</sub>1 (*E. coli* Δ*metK*/pC-*metK*\*, Table S3) lacks the genomic copy of *metK*, but contains a complementary plasmid (pC-*metK*\*) to support normal growth.

The next step is to replace the complementary *metK*\* with a reduced L-methionine binding affinity *metK* variant which is crucial for the MetK mutant characterization. MetK<sup>K265A</sup> and MetK<sup>K269M</sup> mutants with 0.54 mM and 7.1 mM  $K_m$  values, respectively, towards L-methionine [39] are higher than that of the wild-type MetK (MetK<sup>WT</sup>, 0.08 mM). According to the plasmid incompatibility, three plasmids carrying the expression cassette of MetK<sup>WT</sup>(pHL1), MetK<sup>K265A</sup>(pHL2), and MetK<sup>K269M</sup>(pHL3) were transformed into HL<sub>b</sub>1, to replace the pC-*metK*\* for further growth-coupling test (Fig. S3A). However, the chloramphenicol resistance tests and PCR-based genotyping results showed that the pC-*metK*\* was less likely to be replaced by pHL2 and pHL3, compared with pHL1 (Fig. S3B). It was hypothesized that the decreased L-methionine binding affinity of MetK<sup>K265A</sup> and MetK<sup>K269M</sup> dramatically decreased the apparent activity of MetK, making the host to prefer to retain the pC-*metK*\* plasmid for survival. To improve the plasmid exclusion efficiency, FLP recombinase target (FRT) sites in the same orientation flanking Cm<sup>R</sup> and *metK* were introduced into pC-*metK*\* to construct pC-FRT-*metK*\*. An *flp* expression cassette was incorporated into pHL1 to obtain pHL4 for the purpose of looping out the Cm<sup>R</sup> and *metK* cassette in pC-FRT-*metK*\* (Fig. S3A). The exclusion efficiency increased from 0 to over 80% when pHL5 and pHL6 were transformed into HL<sub>b</sub>2 to obtain HL<sub>b</sub>5 and HL<sub>b</sub>6, respectively (Table S2, Fig. S3B). To eliminate the mutants carrying reverse mutation, the *metK* in pHL5 and pHL6 were further confirmed by DNA sequencing. Unexpectedly, a reverse mutation of M269K was observed in HL<sub>b</sub>6, rather than HL<sub>b</sub>5 (Table S3), which could be attributed to the severely decreased activity of MetK<sup>K269M</sup>. In contrast,

the resultant strain HL<sub>b</sub>5 showed severely retarded growth in M9 medium and restored growth, compared to HL<sub>b</sub>4 (Table S3), when L-methionine was supplemented to a final concentration of 0.008 to 0.8 g/L in the medium (Fig. 2B). These results demonstrated that the growth defect caused by the MetK mutant with decreased binding affinity to L-methionine can be restored to some extent by increasing the intracellular L-methionine concentration. However, not all of the mutants with decreased binding affinity could be engineered as biosensor using the established workflow in this section (Fig. S3), such as MetK<sup>K269M</sup>, for the growth-coupling evolution of L-methionine producers. Hence, the range of  $K_m$  value of the mutant needs to be further optimized for better growth-coupling effect.

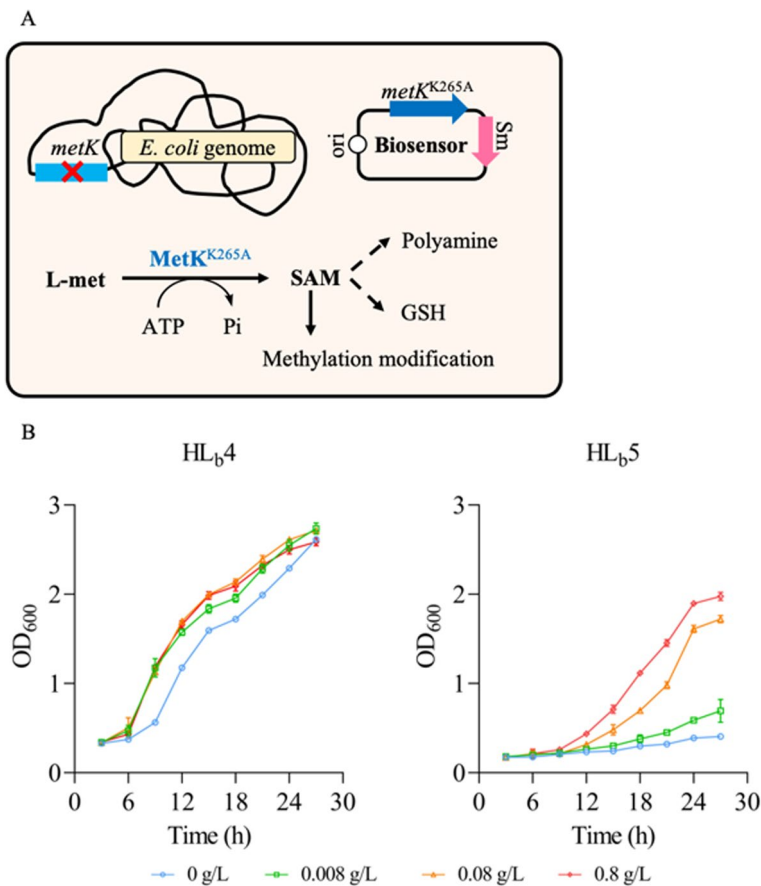


**Fig. 2** MetK-based biosensor for proof of principle. **A** A biosensor plasmid carrying *metK*<sup>K265A</sup> with reduced affinity to L-methionine is expressed in *E. coli* MG1655  $\Delta metK$  to construct a whole-cell biosensor. MetK<sup>K265A</sup> is responsible for the synthesis of the universal methyl donor SAM which is essential for cell growth. **B** The growth curve of HL<sub>b</sub>4 and HL<sub>b</sub>5 (Table S3, *E. coli* MG1655  $\Delta metK$  harboring the biosensor plasmid carrying wild-type *metK* and *metK*<sup>K265A</sup>) in M9 medium supplemented with L-methionine in range of 0–0.8 g/L. All data are shown as mean values. Error bars represent the standard deviation of at least three biological replicates

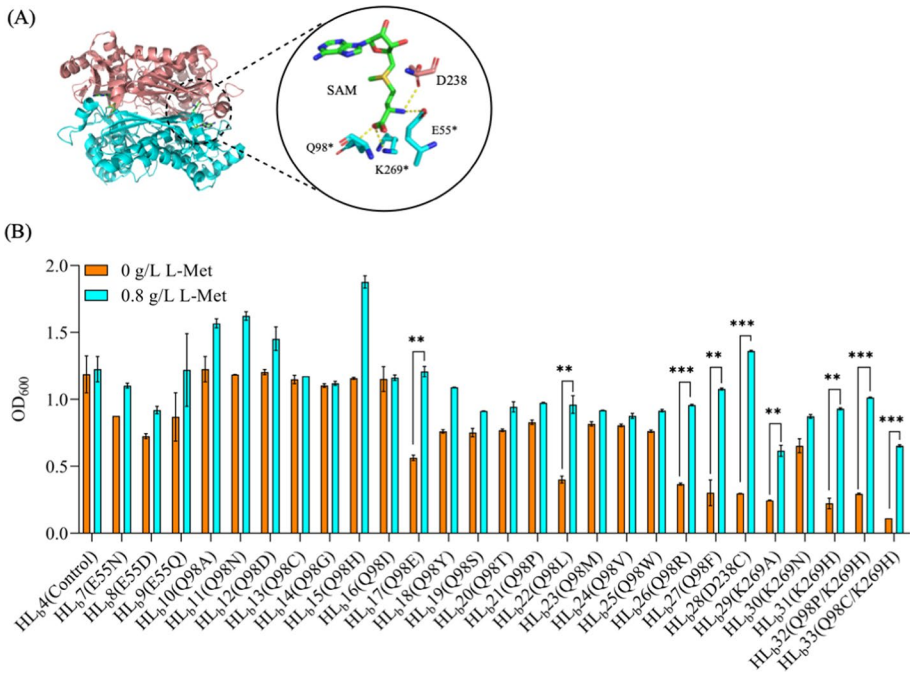


**Fig. 3** Screening and characterization of the MetK-based growth-coupling biosensors. **A** The crystal structure of MetK dimer (PDB ID: 1RG9). The interactions between L-methionine and residues in the active pocket of MetK dimer are presented in detail. **B** Determination of the growth coupling effects of the obtained biosensor candidates which were cultivated for 12 h at 37 °C with or without L-methionine in M9 medium. The information about mutations of MetK in each candidate strain was listed in Table S3. All data are shown as mean values. Error bars represent the standard deviation of at least three biological replicates. The  $p$  value was calculated by Student's two-tailed  $t$ -test (\*\* $p < 0.01$ ; \*\*\* $p < 0.001$ )

### Directed Evolution of MetK for Improving Growth-Coupling Selection

To further identify the better MetK mutants with enhanced metabolic coupling of the intracellular L-methionine availability and cell growth, rational design based on the protein-substrate interaction pattern was implemented in this study. MetK is a homo-tetramer which forms two active pockets at the interface between two subunits (Fig. 3A). Four residues, including E55, Q98, and K269 from one subunit and D238 from another subunit, that interact with L-methionine directly were selected for site-saturated mutagenesis [36] (Fig. 3A). A total of 76 *metK* mutants, corresponding to the above four residues, were constructed and transformed into HL<sub>b</sub>2. The results showed that a large proportion of mutants failed to obtain the expected recombinant strains, because of the severely decreased activity of MetK. Twenty-five out of 75 strains (named as HL<sub>b</sub>7–HL<sub>b</sub>33, Table S3) were finally obtained and validated by antibiotic resistance assay and sequencing (Table S4). These strains were inoculated into 10 mL M9 medium with or without L-methionine addition, to monitor the cell growth (Fig. S4). As shown in Fig. 3B, the growth of strains (HL<sub>b</sub>7–HL<sub>b</sub>33) carrying MetK<sup>Q98E</sup>, MetK<sup>Q98L</sup>, MetK<sup>Q98R</sup>, MetK<sup>Q98F</sup>, MetK<sup>D238C</sup>, MetK<sup>K269A</sup>, and MetK<sup>K269H</sup> single-site mutation was positively related to the concentration of exogenous L-methionine. On the basis of single-site mutation, combinatorial

mutagenesis was further investigated to identify mutants that could be employed to select L-methionine overproducing strains (Table S5, 6, 7). Only two strains (HL<sub>b</sub>32 and HL<sub>b</sub>33) carrying double mutants, MetK<sup>Q98P/K269H</sup> and MetK<sup>Q98C/K269H</sup>, respectively, were demonstrated to have significant growth defect in M9 medium and relieved by exogenous L-methionine addition (Fig. 3B). These results revealed that the proposed strategy is effective to identify novel MetK mutants that could be further adopted as potential biosensors for selecting L-methionine overproducing strains based on cell growth.

## Determination and Expanding of the Dynamic Range of MetK-Based Biosensors Against L-Methionine

The dynamic range of the 9 biosensor strain candidates carrying single or double mutations in MetK which responded to the exogenous L-methionine was further determined. Compared with the wild-type strain HL<sub>b</sub>4 (Fig. S5), the growth of all strains was positively related to the concentration of supplemented L-methionine in the range of 0–0.8 g/L (Fig. 4). Specifically, HL<sub>b</sub>17 and HL<sub>b</sub>33 grew similarly to HL<sub>b</sub>4, when 0.08 g/L L-methionine was supplied in the medium, with the OD<sub>600</sub> reaching 1.0 in 12 h and the change of cell density reaching 1.8 and 2.3-fold, respectively (Fig. 4a, i). Nevertheless, three biosensor strains (HL<sub>b</sub>26, HL<sub>b</sub>27, and HL<sub>b</sub>28) grew normally only when 0.8 g/L L-methionine

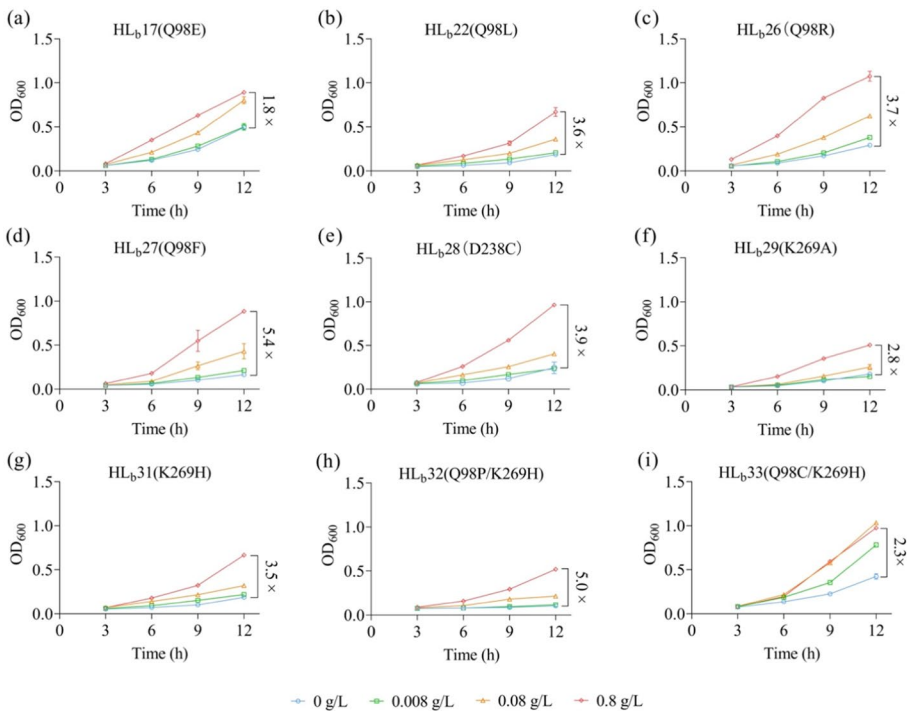


**Fig. 4** Growth curve of *E. coli*  $\Delta metK$  harboring preferred biosensor plasmid in M9 medium supplemented with different concentrations of L-methionine ranging from 0 to 0.8 g/L. **a** HL<sub>b</sub>17 (Q98E); **b** HL<sub>b</sub>22 (Q98L); **c** HL<sub>b</sub>26 (Q98R); **d** HL<sub>b</sub>27 (Q98F); **e** HL<sub>b</sub>28 (D238C); **f** HL<sub>b</sub>29 (K269A); **g** HL<sub>b</sub>31 (K269H); **h** HL<sub>b</sub>32 (Q98P/K269H); **i** HL<sub>b</sub>33 (Q98C/K269H). All data are shown as mean values. Error bars represent the standard deviation of at least three biological replicates

was added in the medium with the change in cell density reaching 3.7-, 5.4-, and 3.9-fold, respectively (Fig. 4c, d, e). Furthermore, the strains HL<sub>b</sub>22, HL<sub>b</sub>29, HL<sub>b</sub>31, and HL<sub>b</sub>32 exhibited more severe retarded growth with the OD<sub>600</sub> reaching less than 0.6 in 12 h (Fig. 4b, f, g, h) in medium with 0.8 g/L L-methionine supplemented. The corresponding change in cell density reached 3.6-, 2.8-, 3.5-, and 5.0-fold, which could be attributed to the lower activity of intracellular MetK than that of the other mutants. Taking the change in cell density and responsive dose into account, the MetK<sup>Q98P/K269H</sup> could be the optimal variant used in the biosensor for further growth-coupling selection of L-methionine over-producers. To further characterize the performance of HL<sub>b</sub>32, the growth curves of HL<sub>b</sub>32 in M9 medium supplemented with 0, 0.008, 0.08, 0.2, 0.4, and 0.8 g/L L-methionine were determined. As shown in Fig. S6, there was no significant difference between cell growth when 0.2, 0.4, and 0.8 g/L L-methionine was supplemented. It was speculated that, for HL<sub>b</sub>32, the maximum uptake rate of L-methionine was achieved with 0.2 g/L L-methionine supplemented. Besides, compared to the cell growth of HL<sub>b</sub>4, the cell growth of HL<sub>b</sub>32 had much longer lag phase and lower cell growth rate even with 0.8 g/L L-methionine added, indicating that HL<sub>b</sub>32 requires higher intracellular L-methionine availability to support faster cell growth as HL<sub>b</sub>4. To determine whether the mutations in *metK* affect its expression level, the relative expression of *metK* in HL<sub>b</sub>4 and HL<sub>b</sub>32 was determined using quantitative real-time PCR (qPCR) and DIA (data-independent acquisition) mass spectrometry. As shown in Fig. S7, there is no significant difference in the relative mRNA expression of *metK* and MetK abundance in HL<sub>b</sub>4 and HL<sub>b</sub>32. These data indicated that the MetK mutant in HL<sub>b</sub>32 has a reduced specific catalytic activity, compared to the wild-type MetK, and HL<sub>b</sub>32 could be a promising biosensor to select mutants with enhanced metabolic flux towards L-methionine biosynthesis.

To further expand the dynamic range of biosensors in response to L-methionine, the gene *yjeH* encoding methionine exporter [40] and *mtnN* encoding S-adenosyl-homocysteine nucleosidase [41] (Fig. 5A) were overexpressed to decrease the intracellular availability of SAM. Biosensors carrying MetK with single mutation MetK<sup>Q98E</sup> or MetK<sup>Q98R</sup>

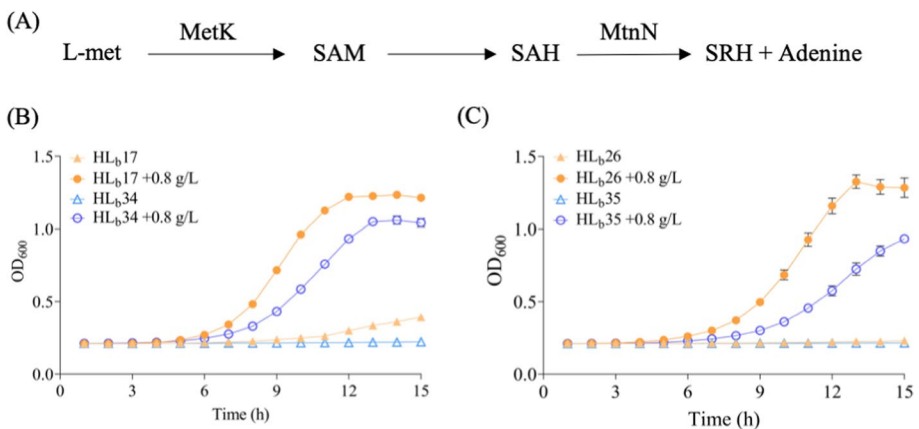


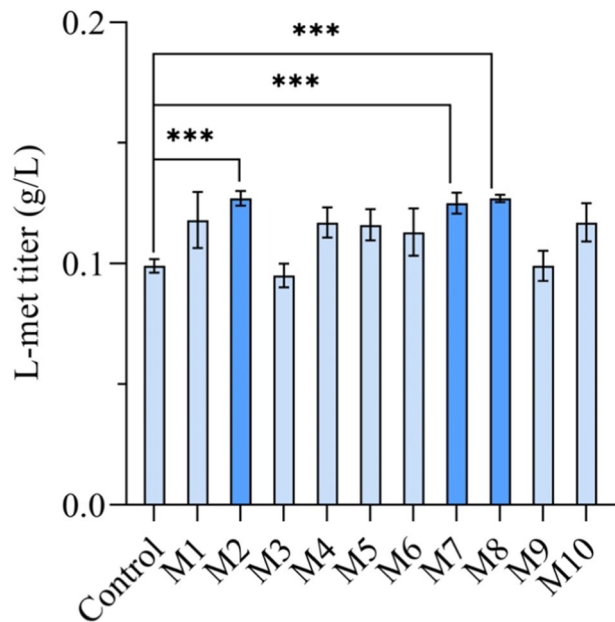
**Fig. 5** Effects of overexpression of *mtnN* on the dynamic range of the biosensor strain HL<sub>b</sub>34 and HL<sub>b</sub>35 towards L-methionine. **A** The catabolic pathway of SAM. **B** The growth curve of biosensor strain HL<sub>b</sub>17 and HL<sub>b</sub>34 in M9 medium with or without L-methionine. **C** The growth curve of biosensor strains HL<sub>b</sub>26 and HL<sub>b</sub>35 in M9 medium with or without L-methionine. All data are shown as mean values. Error bars represent the standard deviation of at least three biological replicates

were taken as examples, since the cell growth of the optimal MetK<sup>Q98P/K269H</sup> was severely retarded even with 0.8 g/L L-methionine supplemented in the medium. As a result, the growth of biosensor strains HL<sub>b</sub>34 ( $\Delta metK$ , carrying *metK*<sup>Q98E</sup>, *mtnN*, and *yjeH*) and HL<sub>b</sub>35 ( $\Delta metK$ , carrying *metK*<sup>Q98R</sup>, *mtnN*, and *yjeH*, Table S3) was significantly retarded in the medium with or without L-methionine, compared to the growth of corresponding strain (HL<sub>b</sub>17 and HL<sub>b</sub>26, respectively) which lacks the overexpression of *mtnN* (Fig. 5B, C). The specific growth rates ( $\mu$ ) of HL<sub>b</sub>17 and HL<sub>b</sub>26 were 0.345 h<sup>-1</sup> and 0.305 h<sup>-1</sup>, respectively, in M9 medium containing 0.8 g/L L-methionine. In contrast, the specific growth rates ( $\mu$ ) of HL<sub>b</sub>34 and HL<sub>b</sub>35 were decreased to 0.285 h<sup>-1</sup> and 0.154 h<sup>-1</sup>, respectively. These results indicated that overexpression of *mtnN* could be an effective strategy to expand the responsive range of the whole-cell biosensors for L-methionine.

### Selection of L-Methionine Overproducing Strain by the Growth-Coupled Biosensor from a Random Mutation Library

The engineered biosensor can detect the intracellular concentration of L-methionine. The intracellular L-methionine availability could be achieved through uptaking from medium and endogenous biosynthesis. Hence, the above optimized whole-cell biosensor (Q98P/K269H) was used to select the strains with enhanced biosynthesis of L-methionine from random mutation libraries. The genomic *metD* was firstly disrupted in strain HL<sub>b</sub>2 to inhibit the uptake of the extracellular L-methionine. The resultant strain HL<sub>b</sub>3 was set as the starting strain to generate random mutation library by ARTP. Then, the optimal biosensor plasmid Q98P/K269H was transformed into the random mutation library and incubated in liquid medium supplemented with antibiotics (streptomycin) for 10 h to enrich the L-methionine overproducing strains and maintain the biosensor plasmid. The culture was then diluted and spread on the SC-M9 solid plate (~ 1000 cells each plate). Ten clones with

**Fig. 6** L-methionine produced by the starting strain and randomly mutated strains selected by the growth-coupled biosensor. All data are shown as mean values. Error bars represent the standard deviation of at least three biological replicates. The *p* value was calculated by Student's two-tailed *t*-test (\*\**p* < 0.01; \*\*\**p* < 0.001)



larger size and faster growth, compared with the control strain HL<sub>b</sub>36 (Table S3), were randomly picked and cultivated for L-methionine production assay. Eight of the ten colonies showed a significant improvement on L-methionine production (Fig. 6). Among these strains, the L-methionine titer of strains M2, M7, and M8 improved by 28.28%, 26.26%, and 28.28%, respectively, compared to the starting strain (HL<sub>b</sub>3). These results indicated that the whole-cell biosensor system can be effectively applied to select L-methionine overproducers from random mutation libraries.

## Discussion

In the present work, a strategy for constructing and optimizing crucial enzymes-based biosensors that can select valuable chemical overproducing strains was proposed. Introducing a variant of the crucial enzyme with low substrate binding affinity into a genomic essential gene defect host leads to a decrease in intracellular availability of the essential metabolite and subsequent inhibition of cell growth. However, this inhibition can be partially restored through supplementing or increasing the intracellular production of the corresponding precursor of the essential metabolite (Fig. 1A). The efficiency of this strategy depends on the substrate binding affinity of the crucial enzyme, which can be fine-tuned through rational design, based on the interaction between the active residues and the precursor of the vital metabolite. The rational design and subsequent application of a binding affinity reduced MetK (S-adenosyl-L-methionine synthetase) in the selection for L-methionine overproducer. This approach successfully led to the isolation of several strains with improved L-methionine production from the random mutation libraries.

Disrupting the genomic copy of essential gene such as *metK* in *E. coli*, which is indispensable for cell growth, poses a significant challenge. To overcome this obstacle, a common strategy of supplying the corresponding metabolite in the medium is applied to recover the growth of the strain lacking the essential gene. However, in some cases, cells may be unable to uptake certain metabolites due to the absence of corresponding transporter protein. For example, *E. coli* lacks the transport proteins capable of transporting SAM across biological membranes [42]. Another efficient strategy is to pre-transform a complementary plasmid carrying the expression cassette of the disrupted essential gene [43]. We pre-transformed a plasmid containing wild-type *metK* expression cassette into *E. coli* MG1655 to maintain normal growth of the genomic *metK* disrupted strain.

Efficient disruption of essential genes using CRISPR-Cas9 technology in a single, markerless step has been achieved. The foremost design principle for genomic *metK* deletion using CRISPR-Cas9 system was to select a spacer sequence (N<sub>20</sub>) from the terminal 30 bp of the deleted fragment to reduce the probability of *metK* in the complementary plasmid functioning as donor. Furthermore, the selected PAM sequence in the complementary *metK* should be replaced by synonymous codons to avoid the unexpected digestion of the complementary plasmid and homologous recombination. Compared to the traditional homology recombination-based [44, 45] or I-SceI-assisted essential gene deletion system [46], the CRISPR-Cas9 system induces double-strand break (DSB) and followed by recombination between the two homology arms for scarless disruption of the essential gene in one step with higher efficiency. This strategy can be adapted for a variety of genome editing applications with appropriate modifications of the pTarget plasmid [30].

To characterize MetK variants and select for hyper-producer, it is necessary to replace the complementary plasmid in the genomic *metK*-deleted host strain with a biosensor

plasmid. Conventionally, plasmid curing could be achieved through the use of plasmids carrying temperature-sensitive origin [47], counter-selective markers [48], or through plasmid incompatibility [49] or the CRISPR-Cas9 system [30]. In this work, plasmid incompatibility was initially applied to replace the complementary plasmid pC-*metK*\* with the biosensor plasmid. However, poor curing efficiency was observed for MetK mutants, possibly due to decreased activity compared to wild MetK. To improve the curing efficiency, the FLP/FRT system was then introduced to loop out the wild-type *metK* and selection marker in the complementary plasmid pC-FRT-*metK*\*. This strategy has successfully improved the curing efficiency to over 80%. However, for some MetK mutants, we failed to obtain the expected recombinant strains carrying biosensor plasmid, which could be attributed to the dramatic decrease of the corresponding mutant's activity.

Structure-based rational design was applied to perturb the direct interaction between substrate and residues in the active pocket of MetK. As a result, seven novel MetK mutants with single-site mutations that exhibited significant growth-coupling effects were identified in *E. coli*  $\Delta$ *metK* in response to L-methionine addition, making them promising candidates for biosensor development. Although we attempted combinational mutagenesis, only two mutants, namely 98C/269H and 98P/269H, were isolated, likely due to the severe decreases in activity of the resultant mutants carrying double or triple mutations. In the circumstances, the host cell exhibited non-growth or lagging growth by keeping both plasmids or inducing the reverse mutation in *metK* variant as observed. Regarding the substrate specificity of the preferred MetK mutants mentioned above, a few studies have shown that MetK can be engineered to transform unnatural substrates such as L-methionine or ATP analogues to S-adenosyl-L-methionine (SAM) analogous that can further modify DNA in vitro [50, 51]. However, it is nearly impossible for the engineered MetK to convert unnatural intracellular metabolites to SAM which is an universal methyl group donor [52, 53] catalyzed by SAM-dependent methyltransferases with strict substrate specificity [54], making specificity an intrinsic superiority of our present biosensor. Furthermore, our strategy can be applied to other crucial enzymes for the rapid development of biosensors, aided by crystal structure and powerful AI tools for protein structure prediction, such as AlphaFold2 [55].

The dynamic range of biosensors is an important parameter for their potential application in high-throughput selection. In this study, the biosensor based on the crucial enzyme immediately converted the intracellular availability of cognate substrate to growth phenotype with high specificity and sensitivity, resulting in an output range of fivefold for the optimal biosensor strain HL<sub>b</sub>32. Quantitative RT-PCR analysis and DIA (data-independent acquisition) mass spectrometry revealed no significant difference in intracellular MetK abundance between HL<sub>b</sub>32 and HL<sub>b</sub>4, indicating the mutations (Q98P and K269H) in MetK reduce its catalytic activity. To further extend the dose–response dynamic range of the whole-cell biosensor and improve its performance, overexpression of the catabolic enzymes consuming the essential metabolite could be useful. The mutation sites selected for MetK engineering are highly conserved and could be adapted from other species. The selected mutation sites, which are highly conserved [56], could be utilized for engineering MetK in other species. Additionally, these mutants could be potentially used in other hosts of interest for the efficient selection of novel microbial cell factories, provided that they can functionally express in the heterologous hosts.

The optimal biosensor proved to be effective in selecting L-methionine overproducing strain from random mutation libraries, leading to the isolation of several strains with significantly improved L-methionine productivity. The titers of isolated L-methionine overproducers are still very low, which could be attributed to the complicated and multilayer regulation of the



L-methionine biosynthesis. Meanwhile, a proportion of false-positives were also identified during the biosensor characterization, which may be caused by reverse mutation in the mutated MetK. Previous reports have shown that although false-positives cannot be completely eliminated, they can be reduced during the biosensor-assisted selection of valuable chemical over-producing strains [17, 27, 57]. To further minimize the effects of false-positives, in addition to the plate-based selection, co-culturing the library strains transformed with the biosensor with an L-methionine auxotrophic strain that harbors an assistant plasmid expressing GFP, employing microdroplet technology to indicate the L-methionine overproducing strains was suggested.

## Conclusions

The present study outlines several strategies for growth-coupled whole-cell biosensor development, including essential gene knockout, plasmid exclusion, proof of concept, and rational design. A whole-cell biosensor responding to L-methionine was successfully developed and characterized. To extend the dose–response dynamic range, the SAM catabolic gene *mtnN* was overexpressed. The growth-coupled biosensor was successfully used to select L-methionine overproducing strains from random mutation libraries. While the L-methionine titer of the isolated strains is much lower than that of the systematically engineered strains [22], additional investigation such as comparative omics analysis and inverse metabolic engineering could provide new clues for the development of L-methionine hyperproducing strains. On the other hand, given the complexity of the L-methionine biosynthesis, further works are needed to improve the abundance and quality of the mutation library in the genome scale to accelerate the development process of L-methionine overproducing strains. Overall, our approach is effective to construct a growth-coupled biosensor and select L-methionine overproducing strain and can be extended to the other crucial enzymes involved in amino acids, vitamins, shikimic acid pathway, and so on to obtain highly valued chemical overproducers.

**Supplementary Information** The online version contains supplementary material available at <https://doi.org/10.1007/s12010-023-04807-0>.

**Author Contribution** JH: conceptualization, investigation, methodology, formal analysis, data curation, visualization, writing—review and editing. JL: investigation, formal analysis, data curation, visualization, writing—review and editing. HD: investigation, review and editing, data curation, visualization. JS: formal analysis, data curation, visualization, writing—review and editing. XY: conceptualization, methodology, supervision, project administration. YZ: conceptualization, methodology, writing—review and editing, supervision, project administration.

**Funding** This work was financially supported by the National Key Research and Development Program of China [2020YFA0908301], the National Natural Science Foundation of China (22208366), and the Tianjin Synthetic Biotechnology Innovation Capacity Improvement Project (TSBICIP-CXRC-019).

**Data Availability** All data generated or analyzed during this study are included in this published article and its supplementary information file.

## Declarations

**Ethics Approval** Not applicable.

**Consent to Participate** Not applicable.

**Consent for Publication** Not applicable.

**Competing Interests** The authors declare no competing interests.

## References

1. Choi, K. R., Jang, W. D., Yang, D., Cho, J. S., Park, D., & Lee, S. Y. (2019). Systems metabolic engineering strategies: Integrating systems and synthetic biology with metabolic engineering. *Trends in Biotechnology*, *37*, 817–837.
2. Lee, S. Y., Kim, H. U., Chae, T. U., Cho, J. S., Kim, J. W., Shin, J. H., Kim, D. I., Ko, Y.-S., Jang, W. D., & Jang, Y.-S. (2019). A comprehensive metabolic map for production of bio-based chemicals. *Nature Catalysis*, *2*, 18–33.
3. Voigt, C. A. (2020). Synthetic biology 2020–2030: Six commercially-available products that are changing our world. *Nature Communications*, *11*, 6379.
4. Ko, Y. S., Kim, J. W., Lee, J. A., Han, T., Kim, G. B., Park, J. E., & Lee, S. Y. (2020). Tools and strategies of systems metabolic engineering for the development of microbial cell factories for chemical production. *Chemical Society Reviews*, *49*, 4615–4636.
5. Fisher, A. K., Freedman, B. G., Bevan, D. R., & Senger, R. S. (2014). A review of metabolic and enzymatic engineering strategies for designing and optimizing performance of microbial cell factories. *Computational and Structural Biotechnology Journal*, *11*, 91–99.
6. Koch, M., Pandi, A., Borkowski, O., Batista, A. C., & Faulon, J. L. (2019). Custom-made transcriptional biosensors for metabolic engineering. *Current Opinion in Biotechnology*, *59*, 78–84.
7. Liu, Y., Liu, Y., & Wang, M. (2017). Design, Optimization and Application of Small Molecule Biosensor in Metabolic Engineering. *Frontiers in Microbiology*, *8*, 2012. <https://doi.org/10.3389/fmicb.2017.02012>
8. Mahr, R., & Frunzke, J. (2016). Transcription factor-based biosensors in biotechnology: Current state and future prospects. *Applied Microbiology and Biotechnology*, *100*, 79–90.
9. Palmer, A. E., Qin, Y., Park, J. G., & McCombs, J. E. (2011). Design and application of genetically encoded biosensors. *Trends in Biotechnology*, *29*, 144–152.
10. Qin, L., Liu, X., Xu, K., & Li, C. (2022). Mining and design of biosensors for engineering microbial cell factory. *Current Opinion in Biotechnology*, *75*, 102694. <https://doi.org/10.1016/j.copbio.2022.102694>
11. Shi, S., Xie, Y., Wang, G., & Luo, Y. (2022). Metabolite-based biosensors for natural product discovery and overproduction. *Current Opinion in Biotechnology*, *75*, 102699.
12. Teng, Y., Zhang, J., Jiang, T., Zou, Y., Gong, X., & Yan, Y. (2022). Biosensor-enabled pathway optimization in metabolic engineering. *Current Opinion in Biotechnology*, *75*, 102696. <https://doi.org/10.1016/j.copbio.2022.102696>
13. Kim, P. J., Lee, D. Y., Kim, T. Y., Lee, K. H., Jeong, H., Lee, S. Y., & Park, S. (2007). Metabolite essentiality elucidates robustness of *Escherichia coli* metabolism. *Proceedings of the National Academy of Sciences of the United States of America*, *104*, 13638–13642.
14. Jang, W. D., Kim, G. B., & Lee, S. Y. (2022). An interactive metabolic map of bio-based chemicals. *Trends in Biotechnology*, *41*, 10–14.
15. Sanchez, S., & Demain, A. L. (2008). Metabolic regulation and overproduction of primary metabolites. *Microbial Biotechnology*, *1*, 283–319.
16. Satishchandran, C., Taylor, J. C., & Markham, G. D. (1990). Novel *Escherichia coli* K-12 mutants impaired in S-adenosylmethionine synthesis. *Journal of Bacteriology*, *172*, 4489–4496.
17. Sun, X., Li, Q., Wang, Y., Zhou, W., Guo, Y., Chen, J., Zheng, P., Sun, J., & Ma, Y. (2021). Isoleucyl-tRNA synthetase mutant based whole-cell biosensor for high-throughput selection of isoleucine over-producers. *Biosensors and Bioelectronics*, *172*, 112783.
18. Orsi, E., Claassens, N. J., Nikel, P. I., & Lindner, S. N. (2021). Growth-coupled selection of synthetic modules to accelerate cell factory development. *Nature Communications*, *12*, 5295.
19. von Kamp, A., & Klamt, S. (2017). Growth-coupled overproduction is feasible for almost all metabolites in five major production organisms. *Nature Communications*, *8*, 15956.
20. Willke, T. (2014). Methionine production—a critical review. *Applied Microbiology and Biotechnology*, *98*, 9893–9914.
21. Zhu, W. Y., Niu, K., Liu, P., Cai, X., Liu, Z. Q., & Zheng, Y. G. (2021). Combining fermentation to produce O-succinyl-L-homoserine and enzyme catalysis for the synthesis of L-methionine in one pot. *Journal of Bioscience and Bioengineering*, *132*, 451–459.
22. Huang, J. F., Shen, Z. Y., Mao, Q. L., Zhang, X. M., Zhang, B., Wu, J. S., Liu, Z. Q., & Zheng, Y. G. (2018). Systematic analysis of bottlenecks in a multibranch and multilevel regulated pathway: The molecular fundamentals of L-methionine biosynthesis in *Escherichia coli*. *ACS Synthetic Biology*, *7*, 2577–2589.
23. Niu, K., Fu, Q., Mei, Z. L., Ge, L. R., Guan, A. Q., Liu, Z. Q., & Zheng, Y. G. (2023). High-level production of L-methionine by dynamic deregulation of metabolism with engineered nonauxotroph *Escherichia coli*. *ACS Synthetic Biology*, *12*, 492–501.

24. Tuo, J., Nawab, S., Ma, X., & Huo, Y. X. (2023). Recent advances in screening amino acid overproducers. *Engineering Microbiology*, *3*, 100066.
25. Mustafi, N., Grunberger, A., Kohlheyer, D., Bott, M., & Frunzke, J. (2012). The development and application of a single-cell biosensor for the detection of l-methionine and branched-chain amino acids. *Metabolic Engineering*, *14*, 449–457.
26. Mohsin, M., & Ahmad, A. (2014). Genetically-encoded nanosensor for quantitative monitoring of methionine in bacterial and yeast cells. *Biosensors and Bioelectronics*, *59*, 358–364.
27. Zheng, B., Ma, X., Wang, N., Ding, T., Guo, L., Zhang, X., Yang, Y., Li, C., & Huo, Y. X. (2018). Utilization of rare codon-rich markers for screening amino acid overproducers. *Nature Communications*, *9*, 3616.
28. Badran, A. H., & Liu, D. R. (2015). Development of potent in vivo mutagenesis plasmids with broad mutational spectra. *Nature Communications*, *6*, 8425.
29. Cherepanov, P. P., & Wackernagel, W. (1995). Gene disruption in *Escherichia coli*: TcR and KmR cassettes with the option of Flp-catalyzed excision of the antibiotic-resistance determinant. *Gene*, *158*, 9–14.
30. Jiang, Y., Chen, B., Duan, C., Sun, B., Yang, J., & Yang, S. (2015). Multigene editing in the *Escherichia coli* genome via the CRISPR-Cas9 system. *Applied and Environmental Microbiology*, *81*, 2506–2514.
31. Maier, R. M., & Pepper, I. L. (2015). Chapter 3 - Bacterial growth. In I. L. Pepper, C. P. Gerba, & T. J. Gentry (Eds.), *Environmental microbiology* (3rd edn.). Academic Press, pp. 37–56. <https://doi.org/10.1016/B978-0-12-394626-3.00003-X>
32. Zhao, J., Yang, Y., Xu, H., Zheng, J., Shen, C., Chen, T., Wang, T., Wang, B., Yi, J., Zhao, D., Wu, E., Qin, Q., Xia, L., & Qiao, L. (2023). Data-independent acquisition boosts quantitative metaproteomics for deep characterization of gut microbiota. *NPJ Biofilms and Microbiomes*, *9*, 4.
33. Wang, L. Y., Huang, Z. L., Li, G., Zhao, H. X., Xing, X. H., Sun, W. T., Li, H. P., Gou, Z. X., & Bao, C. Y. (2010). Novel mutation breeding method for *Streptomyces avermitilis* using an atmospheric pressure glow discharge plasma. *Journal of Applied Microbiology*, *108*, 851–858.
34. Sezonov, G., Joseleau-Petit, D., & D'Ari, R. (2007). *Escherichia coli* physiology in Luria-Bertani Broth. *Journal of Bacteriology*, *189*, 8746–8749.
35. Goodall, E. C. A., Robinson, A., Johnston, I. G., Jabbari, S., Turner, K. A., Cunningham, A. F., Lund, P. A., Cole, J. A., & Henderson, I. R. (2018). The essential genome of *Escherichia coli* K-12. *mBio*, *9*, 02096–02017.
36. Komoto, J., Yamada, T., Takata, Y., Markham, G. D., & Takusagawa, F. (2004). Crystal structure of the S-adenosylmethionine synthetase ternary complex: A novel catalytic mechanism of S-adenosylmethionine synthesis from ATP and Met. *Biochemistry*, *43*, 1821–1831.
37. Datsenko, K. A., & Wanner, B. L. (2000). One-step inactivation of chromosomal genes in *Escherichia coli* K-12 using PCR products. *Proceedings of the National Academy of Sciences of the United States of America*, *97*, 6640–6645.
38. Watt, V. M., Ingles, C. J., Urdea, M. S., & Rutter, W. J. (1985). Homology requirements for recombination in *Escherichia coli*. *Proceedings of the National Academy of Sciences of the United States of America*, *82*, 4768–4772.
39. Taylor, J. C., & Markham, G. D. (2000). The bifunctional active site of S-adenosylmethionine synthetase. Roles of the basic residues. *Journal of Biological Chemistry*, *275*, 4060–4065.
40. Liu, Q., Liang, Y., Zhang, Y., Shang, X., Liu, S., Wen, J., & Wen, T. (2015). YjeH is a novel exporter of L-methionine and branched-chain amino acids in *Escherichia coli*. *Applied and Environmental Microbiology*, *81*, 7753–7766.
41. Cornell, K. A., & Riscoe, M. K. (1998). Cloning and expression of *Escherichia coli* 5'-methylthioadenosine/S-adenosylhomocysteine nucleosidase: Identification of the *pfs* gene product. *Biochimica et Biophysica Acta (BBA) - Gene Structure and Expression*, *1396*, 8–14.
42. Driskell, L. O., Tucker, A. M., Winkler, H. H., & Wood, D. O. (2005). Rickettsial *metK*-encoded methionine adenosyltransferase expression in an *Escherichia coli metK* deletion strain. *Journal of Bacteriology*, *187*, 5719–5722.
43. Parungao, G. G., Zhao, M., Wang, Q., Zano, S. P., Viola, R. E., & Blumenthal, R. M. (2017). Complementation of a *metK*-deficient *E. coli* strain with heterologous AdoMet synthetase genes. *Microbiology*, *163*, 1812–1821.
44. Jasin, M., & Schimmel, P. (1984). Deletion of an essential gene in *Escherichia coli* by site-specific recombination with linear DNA fragments. *Journal of Bacteriology*, *159*, 783–786.
45. Liang, R., & Liu, J. (2008). In-frame deletion of *Escherichia coli* essential genes in complex regulon. *Biotechniques*, *44*, 209–210, 212–205.
46. Yu, B. J., Kang, K. H., Lee, J. H., Sung, B. H., Kim, M. S., & Kim, S. C. (2008). Rapid and efficient construction of markerless deletions in the *Escherichia coli* genome. *Nucleic Acids Research*, *36*, e84.
47. Hashimoto-Gotoh, T., & Sekiguchi, M. (1977). Mutations of temperature sensitivity in R plasmid pSC101. *Journal of Bacteriology*, *131*, 405–412.
48. Reyrat, J. M., Pellicic, V., Gicquel, B., & Rappuoli, R. (1998). Counterselectable markers: Untapped tools for bacterial genetics and pathogenesis. *Infection and Immunity*, *66*, 4011–4017.

49. del Solar, G., Giraldo, R., Ruiz-Echevarría, M. J., Espinosa, M., & Díaz-Orejas, R. (1998). Replication and control of circular bacterial plasmids. *Microbiology and Molecular Biology Reviews*, *62*, 434–464.
50. Dalhoff, C., Lukinavicius, G., Klimasauskas, S., & Weinhold, E. (2006). Synthesis of S-adenosyl-L-methionine analogs and their use for sequence-specific transalkylation of DNA by methyltransferases. *Nature Protocols*, *1*, 1879–1886.
51. Michailidou, F., Klocker, N., Cornelissen, N. V., Singh, R. K., Peters, A., Ovcharenko, A., Kummel, D., & Rentmeister, A. (2021). Engineered SAM synthetases for enzymatic generation of adomet analogs with photocaging groups and reversible DNA modification in cascade reactions. *Angewandte Chemie -International Edition*, *60*, 480–485.
52. Roje, S. (2006). S-Adenosyl-L-methionine: Beyond the universal methyl group donor. *Phytochemistry*, *67*, 1686–1698.
53. Newman, E. B., Budman, L. I., Chan, E. C., Greene, R. C., Lin, R. T., Woldringh, C. L., & D'Ari, R. (1998). Lack of S-adenosylmethionine results in a cell division defect in *Escherichia coli*. *Journal of Bacteriology*, *180*, 3614–3619.
54. Cannon, L. M., Butler, F. N., Wan, W., & Sunny Zhou, Z. (2002). A stereospecific colorimetric assay for (S, S)-adenosylmethionine quantification based on thiopurine methyltransferase-catalyzed thiol methylation. *Analytical Biochemistry*, *308*, 358–363.
55. Jumper, J., Evans, R., Pritzel, A., Green, T., Figurnov, M., Ronneberger, O., Tunyasuvunakool, K., Bates, R., Zidek, A., Potapenko, A., Bridgland, A., Meyer, C., Kohl, S. A. A., Ballard, A. J., Cowie, A., Romera-Paredes, B., Nikolov, S., Jain, R., Adler, J., ... Hassabis, D. (2021). Highly accurate protein structure prediction with AlphaFold. *Nature*, *596*, 583–589.
56. Wang, X., Jiang, Y., Wu, M., Zhu, L., Yang, L., & Lin, J. (2019). Semi-rationally engineered variants of S-adenosylmethionine synthetase from *Escherichia coli* with reduced product inhibition and improved catalytic activity. *Enzyme and Microbial Technology*, *129*, 109355.
57. Stella, R. G., Gertzen, C. G. W., Smits, S. H. J., Gätgens, C., Polen, T., Noack, S., & Frunzke, J. (2021). Biosensor-based growth-coupling and spatial separation as an evolution strategy to improve small molecule production of *Corynebacterium glutamicum*. *Metabolic Engineering*, *68*, 162–173.

**Publisher's Note** Springer Nature remains neutral with regard to jurisdictional claims in published maps and institutional affiliations.

Springer Nature or its licensor (e.g. a society or other partner) holds exclusive rights to this article under a publishing agreement with the author(s) or other rightsholder(s); author self-archiving of the accepted manuscript version of this article is solely governed by the terms of such publishing agreement and applicable law.

## Authors and Affiliations

Jianfeng Huang<sup>1,2</sup> · Jinhui Liu<sup>1,3</sup> · Huaming Dong<sup>1,4</sup> · Jingjing Shi<sup>1,2</sup> · Xiaoyan You<sup>1,3</sup> · Yanfei Zhang<sup>1,2</sup> 

✉ Xiaoyan You  
youxy@tib.cas.cn

✉ Yanfei Zhang  
zhangyf@tib.cas.cn

<sup>1</sup> Tianjin Institute of Industrial Biotechnology, Chinese Academy of Sciences, Tianjin 300308, People's Republic of China

<sup>2</sup> National Center of Technology Innovation for Synthetic Biology, Tianjin 300308, People's Republic of China

<sup>3</sup> Henan Engineering Research Center of Food Microbiology, College of Food and Bioengineering, Henan University of Science and Technology, Luoyang 471023, People's Republic of China

<sup>4</sup> School of Environmental Ecology and Biological Engineering, Wuhan Institute of Technology, Wuhan 430205, People's Republic of China